

# The effective dissipation in Nb/AIO<sub>x</sub>/Nb Josephson tunnel junctions by return current measurements

R. Cristiano, L. Frunzio, and C. Nappi<sup>a)</sup>

*Istituto di Cibernetica del CNR, Arco Felice, Naples, Italy and INFN sez. Napoli, Naples, Italy*

M. G. Castellano and G. Torrioli

*Istituto di Elettronica dello Stato Solido del CNR, Rome, Italy and INFN sez. Roma, Rome, Italy*

C. Cosmelli

*Università di Roma "La Sapienza", Rome, Italy and INFN sez. Roma, Rome, Italy*

(Received 20 June 1996; accepted for publication 12 February 1997)

Measurements of temperature dependence of the return current in high quality Nb/AIO<sub>x</sub>/Nb Josephson junctions are presented. From the experimental data, we obtain the effective resistance, i.e., the effective dissipation, for the retrapping process, according to the generalized resistively shunted junction model proposed by Chen, Fisher, and Leggett. We present a careful analysis, based on a comparison between the measured temperature dependencies of both the return and the quasiparticle tunneling current. We find that the junction subgap conductance, which includes the quasiparticle and the quasiparticle-pair interference terms, is responsible for the return process. The measurements have been performed on various samples, in a wide range of critical current densities from 50 to 2250 A/cm<sup>2</sup>, covering different damping regimes and spanning over the high and low temperature limits. Junctions with low critical current density show ideal dissipation which makes the return current scale with temperature according to the BCS exponential behavior without flattening out effects. This result may be relevant for the possible use of Nb/AIO<sub>x</sub>/Nb junctions in macroscopic quantum coherence experiments, which strongly require a very low dissipation.

© 1997 American Institute of Physics. [S0021-8979(97)04310-7]

## I. INTRODUCTION

Very recently new experimental efforts have been undertaken to observe macroscopic quantum coherence (MQC) effects. As it is well known, these investigations belong to a long dated and fundamental debate on the validity of quantum mechanics at macroscopic level. The rf-superconducting quantum interference device (SQUID), a superconducting loop interrupted by a Josephson tunnel junction (JTJ), has been proposed as a possible experimental system for the study of MQC.<sup>1-10</sup> Since dissipation plays a crucial role in destroying the quantum coherence, the ideal Josephson junction for such experiments must have very low dissipation.

In the past decade, the fabrication technology of JTJs based on the Nb/AIO<sub>x</sub>/Nb trilayer has been developed to a very high quality standard. Nowadays experiments down to 1 K with ideal junctions are performed, in which high subgap resistances, and consequently very low related dissipations, are observed. By this technology, it is possible to realize junctions in a very wide range of transparencies, with a "hardware" spanning through various dissipation regimes. Nb/AIO<sub>x</sub>/Nb junctions offer, among others, the advantage of entering the quantum regime at higher temperatures, thanks to the small AIO<sub>x</sub> dielectric constant. This leads to a smaller specific capacitance and thus to higher plasma frequencies and crossover temperatures between the thermal and the quantum regime with respect to Nb-based junctions with a Nb<sub>x</sub>O<sub>y</sub> barrier. Furthermore, it is well known that Nb/AIO<sub>x</sub>/Nb JTJs have very good properties against me-

chanical and thermal stresses. Accordingly, this technology is highly indicated to produce ideal and very reliable devices able to operate in the same conditions many times for a long period. All these properties increase the possibility to obtain optimal parameters to perform a MQC experiment.

It is worth mentioning that also Pb-In-Au based Josephson junctions exhibit good properties.<sup>11</sup> In particular, a low specific capacitance marks them out due to the In<sub>2</sub>O<sub>3</sub> oxide that largely composes the tunneling barriers.<sup>12,13</sup> However, such properties are not superior to those of the Nb/AIO<sub>x</sub>/Nb trilayer, whereas a much more critical and difficult fabrication technology is certainly involved. For this reason, the Pb-In-Au technology has been dropped during the past decade.

Although it is still not clear which effective dissipation should be used and whether it can be extracted from current-voltage characteristics, it was claimed that the determination of the dissipation of the junction from the return current data can provide a reliable estimate of the dissipation for MQC experiments. In fact, the return current observed in experiments on Nb/Nb<sub>x</sub>O<sub>y</sub>/PbIn junctions<sup>9,10</sup> closely follows the theoretical predictions for the ideal-tunnel-junction model proposed by Chen, Fisher, and Leggett<sup>14</sup> (thereafter referred to as CFL), demonstrating that, for sufficiently high quality junctions, the dissipation in the return process is dominated by the tunnelling of thermally excited quasiparticles.

In this work, we present measurements of the return current in high quality Nb/AIO<sub>x</sub>/Nb Josephson junctions, which can lead to a better understanding of the effective damping of the retrapping process. Moreover, our results can also be useful in view of the possible use of high quality

<sup>a)</sup>Electronic mail: nappi@fiscn.cib.na.cnr.it

Nb/AlO<sub>x</sub>/Nb Josephson junctions in MQC experiments. We carried out measurements on several samples with different critical current densities, exploring various dissipation regimes. For some samples, the measurements have been performed from about 9 down to 1 K, in order to cover a wide temperature interval. Our results show that Nb/AlO<sub>x</sub>/Nb junctions achieve such a high quality that the return process is dominated by the intrinsic junction resistance.

The article is organized as follows: in Sec. II, we briefly report the problem of the effective dissipation and in Sec. III, we summarize the main results of the CFL model which is used in our work; in Sec. IV, we report the experimental results and their analysis; in Sec. V, we briefly discuss the conclusions.

## II. THE PROBLEM OF THE EFFECTIVE DISSIPATION

In a rf-SQUID, the magnetic flux linked to the loop,  $\Phi$ , plays the role of a macroscopic variable in a 1D potential,  $U(\Phi)$ , determined by the loop inductance,  $L$ , the external magnetic field flux,  $\Phi_{\text{ext}}$ , and the Josephson critical current of the JTJ,  $I_c$ :

$$U(\Phi) = \frac{1}{2L} (\Phi - \Phi_{\text{ext}})^2 - \frac{I_c \Phi_0}{2\pi} \cos \frac{2\pi\Phi}{\Phi_0}, \quad (1)$$

where  $\Phi_0 = h/2e$  is the flux quantum. With the notation  $\beta_L = 2\pi LI_c/\Phi_0$ , Eq. (1) represents a symmetric two-well potential for  $\Phi_{\text{ext}} = \Phi_0/2$  and  $1 < \beta_L < 5\pi/2$ . In the analogy with mechanics,  $\Phi$  is the coordinate of a particle moving in the same potential. The particle can be thermally activated or can tunnel between the two distinct states, which differ only by the direction of the macroscopic screening current flowing in the loop. If the dissipation in the system is negligible, the particle is predicted to coherently oscillate between these states, that is it tunnels performing periodic inversions in the direction of the current in the loop.<sup>2,3</sup> The tunneling process is dominant if the rf-SQUID is operated at low temperature. The onset temperature at which the oscillations may be observed scales with the junction resistance<sup>2,3</sup> so very low dissipation junctions in the rf-SQUID are needed for the observation of the MQC. In this framework, the study of the dissipation in the single junction is an important issue to establish the feasibility of this experiment at accessible low temperatures.

To this end, it is often useful to follow in details the mechanical analogy of a single JTJ. In this case, the macroscopic variable analogous to the coordinate of the particle is  $\varphi$ , the difference in the order parameter between the two junction electrodes.  $\varphi$  is now in a tilted “washboard” 1D potential. The dissipative and the noise terms added to the tilting bias current represent the junction interaction with the environment, whose nature is both thermal and quantum. The quantum regime is dominant below the crossover temperature  $T_{co} = \hbar \omega_p / 7.2 k_B$ ,<sup>15</sup> where  $\omega_p$  is the Josephson plasma frequency.

Several experiments have been performed on JTJs to understand the thermal activation and the quantum tunneling from the zero voltage (locked) state to the finite voltage (running) state. The aim of the experiments is to determine the

dissipation source and to investigate about its magnitude, temperature, and frequency dependencies.<sup>16–31</sup> Nevertheless, a considerable disagreement remains on this subject, partially due to the different experimental techniques that were adopted. In Ref. 16, a very useful method was introduced, that is the measurement of the probability distribution of switching currents and the dependence of its width from temperature. Authors of Refs. 18 and 19 find a good agreement between experiment and theory by using the normal state tunneling resistance,  $R_N$ , to evaluate the damping parameter in the framework of the resistively shunted junction (RSJ) model. However, the Nb/Nb<sub>x</sub>O<sub>y</sub>/Nb junctions which they use have nonideal I–V characteristics. This could explain why they can use the  $R_N$  value in the damping parameter expression.

In fact, in experiments with higher quality Nb/Nb<sub>x</sub>O<sub>y</sub>/PbIn junctions,<sup>20–23</sup> in the thermal activation regime, it is possible to relate the dissipation to the subgap resistance. A discrepancy of about one order of magnitude is observed. Thus the effective dissipation is attributed to non-tunneling processes of thermally activated quasiparticles. In a more complete series of experiments on thermal activation and quantum tunneling regimes,<sup>24–28</sup> the external loading circuit is significantly influencing the effective dissipation. This was clearly confirmed by other experiments on Nb/Nb<sub>x</sub>O<sub>y</sub>/PbInAu JTJs.<sup>29,30</sup>

In all the experiments mentioned above, the effective resistance is extracted from measurements of the decay rate,  $\Gamma$ , of the locked state. Actually, the effective dissipation involved in the escape from the zero voltage state is only weakly related to  $\Gamma$ .<sup>15,32–35</sup> In the thermal regime,  $\Gamma$  depends exponentially on the potential energy barrier height,  $\Delta U$ , and the prefactor only is affected by the damping. On the other hand, in the quantum regime, the  $\Gamma$  dependence on the effective dissipation is exponential, but the evaluation of  $\Delta U$  with a small error can produce large deviations in the inferred values of the dissipation parameter. To further complicate the scenario, the external load can shunt the junction at microwave frequencies with a characteristic impedance of the order of the vacuum impedance,  $377 \Omega$ , so that the effective dissipation of the system has a lower bound. Since the escape process involves motion at or near  $\omega_p$ , the observed frequency dependence of the damping<sup>24–30</sup> is not due to the intrinsic junction resistance. Experiments on the incoherent relaxation by tunneling in SQUIDs seem to confirm that the effective dissipation is not related to the intrinsic junction resistance. Also in this case the effect of the experimental set-up is dominating and leads to a parallel, nonidentified shunt, which becomes the effective dissipation source.<sup>36–38</sup>

As already mentioned in the Introduction, it has been proposed to evaluate the effective dissipation using the re-trapping in the zero voltage state from the running state.<sup>14</sup> In fact, both the deterministic return current,  $I_r$ , and  $\Gamma_r$ , when the effect of fluctuations is also considered, have a strong dependence on  $R$ .<sup>39</sup> Moreover, it is well known that in very hysteretic junctions  $I_r$  is much smaller than  $I_c$ , so that the washboard potential, at this bias value, has very low tilting and is similar to the two-well potential of the rf-SQUID. The

frequency spectrum of the particle motion is dominated by frequencies much lower than  $\omega_p$  and then the junction is not shunted by the external loading circuit.

In the past, the attention was focused on the decay rate of the running state in presence of fluctuations. Several theoretical works reported various attempts to investigate this problem<sup>39-43</sup> and some preliminary experiments were also performed.<sup>44-46</sup> Recently, these attempts were again undertaken on high quality Nb/Nb<sub>x</sub>O<sub>y</sub>/PbIn junctions,<sup>9,10</sup> showing a qualitative agreement with the hypothesis that the effective dissipation is dominated by the tunneling of thermally excited quasiparticles.

It is worth mentioning the experimental work of Ref. 46 on Sn/SnO<sub>x</sub>/Sn junctions, pointing out problems due to the external loading. In that case, the return switchings take place at a relatively high subgap voltage, so that probably high frequency components are important in determining the effective resistance.

### III. THEORETICAL FRAMEWORK FOR THE RETURN CURRENT

The behavior of a real JTJ is approximated in the RSJ model<sup>47</sup> by an ideal JTJ, which carries a current  $I = I_c \sin \varphi$ , parallel with a voltage independent resistance,  $R$ , and a capacitance,  $C$ . The current balance for this circuit biased by an external current generator corresponds to the equation of motion for the macroscopic variable  $\varphi$ :

$$\frac{d^2\varphi}{d\tau^2} + \frac{1}{\omega_p RC} \frac{d\varphi}{d\tau} - \alpha + \sin \varphi = 0, \quad (2)$$

where  $\tau = \omega_p t$  is the time in unit of  $\omega_p^{-1}$  where  $\omega_p = (2\pi I_c / \Phi_0 C)^{1/2}$  and  $\alpha = I/I_c$  is the normalized bias current flowing through the junction. If the damping parameter,  $\beta_j = (\omega_p RC)^{-1} < 1$ , two solutions of Eq. (2) exist: the locked state, corresponding to the phase confined in a potential minimum in which the oscillation frequency of the phase difference is approximately  $\omega_{osc} = \omega_p(1 - \alpha^2)^{1/4}$ , and the running state, corresponding to a monotonically increasing phase difference with an average voltage  $V = (\Phi_0/2\pi) \times (d\varphi/dt)$ . For  $\alpha > 1$ , only the running state is possible. As the bias current is reduced from a value  $\alpha > 1$  down to  $\alpha < 1$ , a critical value  $\alpha_r = I_r/I_c$  will be reached. The running state is characterized by a balance between the energy,  $\Phi_0 I$ , fed into the system by the external bias current and the energy dissipated per cycle,  $W$ . Near  $\alpha_r$ , the particle reaches the top of the potential barrier with less and less kinetic energy. The junction is going to be retrapped in the zero voltage state. For  $\beta_j \ll 1$ , in the RSJ model, this condition is satisfied when the bias current is:

$$I_r^{RSJ} = \frac{4}{\pi} \frac{I_c}{\omega_p RC}. \quad (3)$$

It is possible to substitute in the RSJ model, Eq. (2), the voltage independent  $R$  value with a resistance,  $R_{eff}$ , deriving from both the quasiparticle current and the quasiparticle-pair interference current.<sup>14</sup> In an ideal junction, the quasiparticle current is<sup>48</sup>

$$I_{qp}^{BCS}(V, T) = \frac{1}{R_N} \int_{-\infty}^{\infty} n_L(V', T) n_R(V' - V, T) \times [f(V' - V, T) - f(V', T)] dV', \quad (4)$$

where  $n_{L(R)}$  is the BCS quasiparticle state density for the  $L(R)$  electrode and  $f(V, T)$  is the Fermi function. The quasiparticle-pair interference current  $I_{J2}$  is given by a similar equation<sup>48</sup> where the BCS quasiparticle state densities are substituted with the BCS pair state densities.

$R_{eff}$  can be cast in the form:<sup>14</sup>

$$\frac{1}{R_{eff}} = \frac{1}{R_{qp}} + \frac{\varepsilon}{R_{J2}} \cos \varphi, \quad (5)$$

where  $R_{qp}$  and  $R_{J2}$  are the frequency independent low-voltage quasiparticle and quasiparticle-pair interference resistances respectively and  $\varepsilon = +1$ .<sup>48</sup>

An expression corresponding to the Eq. (3) can be obtained by the energy balance condition:

$$W = \int_0^{T_0} \frac{\dot{\varphi}^2}{R_{eff}} dt = \int_{-\pi}^{\pi} \frac{\dot{\varphi}}{R_{eff}} d\varphi = \Phi_0 I, \quad (6)$$

where  $T_0$  is the traversal time of the well.

In the limits of  $\beta_j \ll 1$  and  $\alpha \ll 1$ ,  $d\varphi/dt$  assumes for the retrapping process (zero kinetic energy at all potential maxima) the following form:<sup>14</sup>

$$\frac{d\varphi(t)}{dt} = 2\omega_p \cos \frac{\varphi(t)}{2}. \quad (7)$$

The Fourier components of Eq. (7) have frequencies in the range of  $0 < \omega \leq \omega_p$ , with dominant very low frequency components as can be shown by a spectral analysis.

If  $\hbar \omega_p \ll \Delta_i$  and  $k_B T$ , a good approximation is

$$R_{qp} = \frac{V_r}{I_{qp}^{BCS}(V_r, T)}, \quad (8a)$$

$$R_{J2} = \frac{V_r}{I_{J2}^{BCS}(V_r, T)}, \quad (8b)$$

$$V_r \leq \frac{2}{\pi^2} \Phi_0 \omega_j, \quad (8c)$$

where  $V_r$  is the retrapping voltage.<sup>48</sup> In similar conditions, CFL obtained an expression corresponding to Eq. (3) for the return current:

$$I_r = \frac{4}{\pi} \frac{I_c}{\omega_p C} \left( \frac{1}{R_{qp}} + \frac{1}{3R_{J2}} \right) = \frac{16}{3\pi} \frac{I_c}{\omega_p R_{qp} C}. \quad (9)$$

This equation, through  $R_{qp}$ , contains a very entangled implicit dependence on  $V$  and  $T$ , see Eqs. (4) and (8). Introducing a simple approximation for the quasiparticle and the quasiparticle-pair interference currents in the high temperature limit ( $\hbar \omega_p < k_B T < \Delta$ ):

$$I_{qp}^{CFL}(V, T) = I_{J_2}^{CFL}(V, T) = \frac{V}{R_N} \left[ \ln \left( \frac{2k_B T}{|V|} \right) - \gamma \right] \frac{\Delta}{k_B T} \times \exp \left( - \frac{\Delta}{k_B T} \right). \quad (10)$$

CFL obtained an analytic expression for the return current:

$$I_r^{CFL} = \frac{8}{3\pi^2} \frac{\Phi_0 \omega_p}{R_N} \left[ \ln \left( \frac{\pi k_B T}{\hbar \omega_p} \right) - a \right] \frac{\Delta}{k_B T} \exp \left( - \frac{\Delta}{k_B T} \right), \quad (11)$$

where  $\gamma \approx 0.577$  is the Euler constant and  $a$  is defined as

$$a = \gamma + \frac{6}{\pi^2} \int_{-\infty}^{\infty} \frac{x^2 \ln x}{\sinh^2 x} dx = 0.237. \quad (12)$$

In the low temperature limit ( $k_B T < \hbar \omega_p < \Delta$ ), using the quantum relationships corresponding to Eqs. (2) and (10) and the same energy balance method, the authors of Ref. 11 obtained the following expression for the return current:

$$I_r^{CFL} = \frac{2}{\pi} \frac{\Phi_0 \omega_p}{R_N} \left( \frac{2\Delta}{\hbar \omega_p} \right) \exp \left( - \frac{2\pi\Delta}{\hbar \omega_p} \right). \quad (13)$$

Equations (9), (11), and (13) are obtained from noiseless equations. Thermal and quantum fluctuations leads to an additive contribution to  $I_r$ . This contribution can be estimated from the maximum of the probability distribution of the noise induced retrapping processes. The probability distribution of the normalized return currents,  $P(\alpha)$ , for a finite normalized sweep rate,  $d\alpha/dt$ , is obtained from the decay rate,  $\Gamma(\alpha)$ , by

$$P(\alpha) = -\Gamma_r(\alpha) \left( \frac{d\alpha}{dt} \right)^{-1} \times \exp \left\{ - \int_1^\alpha \Gamma_r(\alpha') \left( \frac{d\alpha'}{dt} \right)^{-1} d\alpha' \right\}. \quad (14)$$

For thermal fluctuations, an analytic expression for  $\Gamma_r(\alpha)$  has been given by Ref. 39:

$$\Gamma_r(\alpha) = (\alpha - \alpha_r) \frac{I_c}{\sqrt{\pi C k_B T}} \exp \left\{ - (\alpha - \alpha_r)^2 \frac{I_c^2 R_{\text{eff}}^2 C}{k_B T} \right\}. \quad (15)$$

The maximum of  $P(\alpha)$  is given by the solution of the following equation in  $\alpha$ :

$$(\alpha - \alpha_r)^2 \left[ \frac{I_c}{\sqrt{\pi C k_B T}} \exp \left\{ - (\alpha - \alpha_r)^2 \frac{I_c^2 R_{\text{eff}}^2 C}{k_B T} \right\} \left( \frac{d\alpha}{dt} \right)^{-1} + 2 \frac{I_c^2 R_{\text{eff}}^2 C}{k_B T} \right] = 1 \quad (16)$$

which provides the additive contribution,  $(\alpha - \alpha_r)$ .

#### IV. EXPERIMENTAL RESULTS AND DISCUSSION

The data presented in this work refer to Nb/AlO<sub>x</sub>/Nb trilayer junctions fabricated by different processes with different tunnel barrier transparencies. Many samples were measured to check the consistency of the results. Here we

TABLE I. Main parameters of the observed junctions.

Sample	Area ( $\mu\text{m}^2$ )	$J_c$ (A/cm <sup>2</sup> )	$R_N$ ( $\Omega$ )	$C_s$ (fF/ $\mu\text{m}^2$ )	$V_m$ (mV)	$\Delta(T=0)$ (mV)	$T_c$ (K)
a	113	52	31.67	66	81	1.450	8.750
b	138	85	13.75	66	90	1.425	8.945
c	16	1068	9.10	50	79	1.425	8.900
d	25	2250	3.03	66	26	1.350	8.450

shall refer only to the more representative ones. The sample (b) has been fabricated by a process developed at the Istituto di Cibernetica del CNR (IC-CNR) and previously presented in Ref. 49; The sample (c) has been prepared at the Istituto di Elettronica dello Steto Solido CNR (IESS-CNR) as described in Ref. 31 and other two (a) and (d) have been realized at the Electrotechnical Laboratory of Tsukuba in Japan as reported in Ref. 50. In Table I, the main junction parameters are listed. The junctions fall in three categories: low, intermediate, and higher  $J_c$ . According to this classification, a rather different temperature dependence of the return current has been observed.

The  $V_m$  quality factor for all the samples is generally high, decreasing as  $J_c$  increases, and testifies to the good quality of our samples. In order to allow the assessment of the quality, we report the I–V characteristics (thick lines) of the sample a, Fig. 1(a) and sample d, Fig. 1(b), respectively, those with the lowest and the highest  $J_c$ . In Figs. 1(a) and

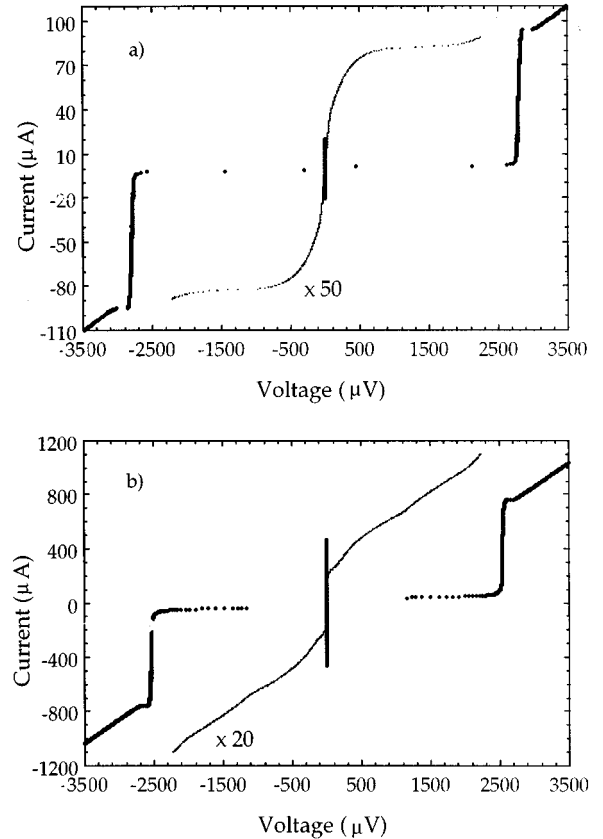


FIG. 1. Experimental current vs voltage characteristics for sample a (a) and sample d (b) at  $T=4.2$  K. The thin lines represent the quasiparticle current of the same samples magnified by the indicated factor.

TABLE II. Energy scales in the performed temperature ranges.

Sample	$T_{\min}-T_{\max}$ (K)	$k_B T$ ( $\mu\text{eV}$ )	$\hbar \omega_p$ ( $\mu\text{eV}$ )	$k_B T / \hbar \omega_p$
a	2.1–4.2	183–365	106–102	1.73–3.58
b	2.8–8.7	242–751	137–35	1.77–21.46
c	1.3–4.2	109–361	481–462	0.23–0.78
d	1.1–4.2	95–365	702–670	0.14–0.54

1(b) we also present the experimental quasiparticle current characteristics (thin lines) magnified by an indicated factor. These curves have been obtained by applying suitable magnetic fields to suppress the  $I_c$  and Fiske steps.

The junction specific capacitances,  $C_s$ , have been obtained by the voltage position measurements of the Fiske steps and the critical temperature,  $T_c$ , recording the appearance of the Josephson current.

The measurements have been performed in Mumetal shielded dewars in two different ranges of temperature: from 4.2 down to about 1 K, in a pumped bath of liquid helium and from 4.2 up to 9 K in the cold vapors of the bath. Calibrated germanium thermometers heat sunk to the copper holder, which contains the samples and the filters, have been used to read the temperature. Filtering from external noise has been provided through cold RC low pass filters mounted as close as possible to the JTI on each lead connecting it to the acquisition electronics. These filters have a cutoff frequency of about 50 kHz.

In this experimental configuration,  $I_c$  and  $I_r$  have been measured at different temperatures. For the samples a and d, measurements of probability distributions of the switching currents  $I_c$  have also been performed. These measurements have been presented elsewhere.<sup>51</sup> They were used in this context as a test of the noise rejection of the experimental set-up. The analysis of the distribution of the return current  $I_r$  is a much more entangled task due to the experimental problems in resolving very low current amplitudes, and due to the difficulties in comparing the data with the two available theories.<sup>14,39</sup> This work is presently in progress.

$I_r$  and  $I_c$  for the other samples were measured by directly reading at the oscilloscope, using a comparator circuitry, in order to amplify the current. During these measurements, the  $dI/dt$  quantity was also recorded. In Table II are reported, for each sample, the explored temperature interval and the energy associated with the plasma frequency. It is possible to see that the samples with the lower  $J_c$  are in the high temperature limit ( $k_B T / \hbar \omega_p > 1$ ), in the whole explored temperature region. The sample with intermediate  $J_c$  value is in an intermediate temperature limit ( $k_B T / \hbar \omega_p \leq 1$ ). Finally, the sample with the highest  $J_c$  is in the low temperature limit ( $k_B T / \hbar \omega_p < 1$ ).

In Fig. 2, experimental results for  $I_r$  are reported for these four JTJs. Since the junctions had different areas and  $J_c$ , the data were multiplied by  $R_N$ . Samples a and b, which were in the high temperature limit ( $\hbar \omega_p < k_B T < \Delta$ ) show an increasing behavior from  $T_c$  down to about 6 K, whereas an exponential decrease is observed down to 2 K. No flattening out effects are observed for these junctions. On the contrary,

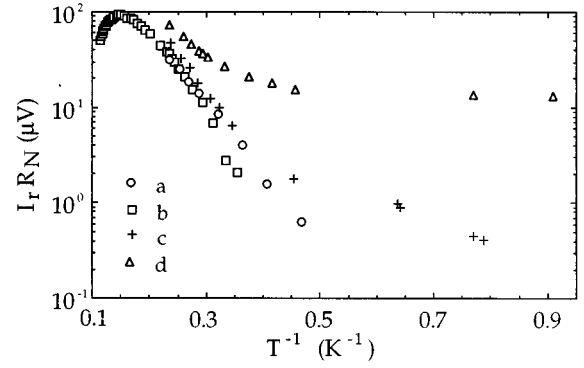


FIG. 2. Semilogarithmic plot of the experimental return current times the normal resistance vs the inverse of the temperature. Error bars are included in the symbols.

flattening out of  $I_r$  is shown by the higher  $J_c$  junctions, which were no longer in the high temperature limit.

### A. Low $J_c$ junctions

These junctions are the most interesting from the point of view of their possible use in MQC experiments. Down to 2 K, they do not exhibit any flattening out of both  $I_r$  and  $I_{qp}$  at low voltages.  $I_{qp}$  was also measured down to about 1.2 K without observing any flattening out. On these samples, we have then performed a very stringent comparison between these  $I_r$  and  $I_{qp}$  in order to determine the effective dissipation responsible for the  $I_r$  switching.

The procedure adopted was the following. By using Eq. (16), in which  $\alpha_r$  is the deterministic expression given by Eq. (3), we obtain  $R_{\text{eff}}$  by fitting the experimental current values at various temperatures. Since  $I_c$ ,  $C$ , and  $T$  were independently measured,  $R_{\text{eff}}$  is, in this procedure, the only fitting parameter.

Equation (9) provides the relationship between  $R_{\text{eff}}$  and  $R_{qp}$ , that is  $R_{qp} = 4R_{\text{eff}}/3$ , which includes the quasiparticle-pair interference contribution as discussed in Sec. III. Thus, the current is given by  $I = 3V_r/4R_{\text{eff}}$ , where  $V_r$  is the experimental retrapping voltage. These latter current values are finally compared with the measured  $I_{qp}(V_r)$  values as well as with the theoretical BCS predictions for  $I_{qp}$  in the same temperature range.

On one side, the comparison between the measured and theoretical  $I_{qp}$  sets the junction quality and gives us information about possible spurious conduction channels that may shunt the intrinsic junction resistance, at very low temperatures. On the other side, the agreement between the current values obtained with the procedure described above and the measured  $I_{qp}$  values allows to state that the quasiparticle and quasiparticle-pair interferences are effectively responsible for the return switching to the zero voltage state.

Figure 3 refers to measurements on sample a. In Fig. 3(a) open circles are the measured  $I_r$  values used in Eq. (16) to obtain  $R_{\text{eff}}$ . In order to explicitly check the consistency of our procedure, we have inserted in Eq. (3) the so computed values of  $R_{\text{eff}}$  to calculate the noiseless  $I_r$  values, reported as open squares in Fig. 3. As it can be seen, the agreement with

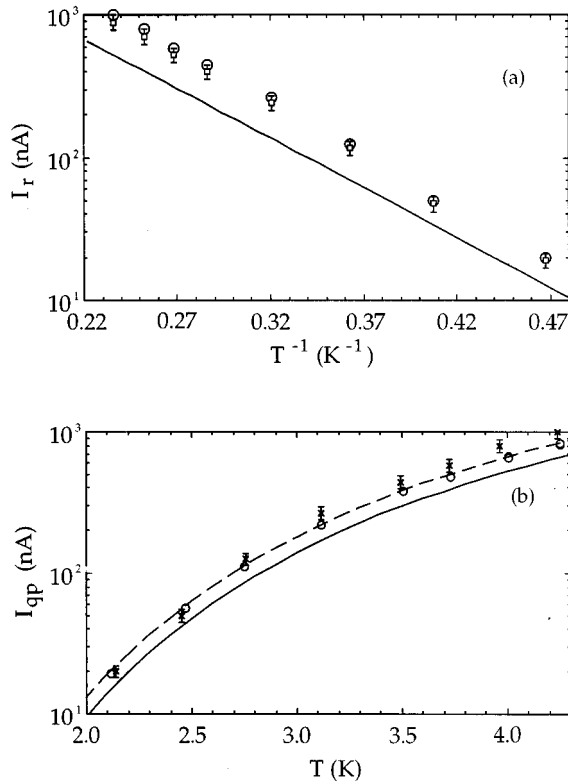


FIG. 3. (a) Semilogarithmic plot of the return current vs the inverse of the temperature for sample a. The open circles are the experimental results including the error bars. The solid line and the open squares represent, respectively, the noiseless theory of Eq. (11) and the noiseless return current evaluated by Eq. (3). (b) Semilogarithmic plot of the quasiparticle current vs the temperature for sample a. The open circles are the measured values of  $I_{qp}$  at  $V = V_r = 0.1$  mV. The crosses represent the values of  $I_{qp}^{\text{fit}}$ . Error bars, if not reported, are included in the symbols. The solid line is the predicted temperature dependence of  $I_{qp}$  at  $V = V_r$  and  $\Delta = 1.45$  mV. The dashed line shows the same dependence with  $V = 0.13$  and  $\Delta = 1.41$  mV.

the experimental  $I_r$  values is quite good indicating that the effect of thermal fluctuations becomes relevant only at high temperatures where indeed fluctuations are expected to play the major role. For the sake of completeness, we performed the same comparison of Ref. 10 plotting the result of Eq. (11) as a solid line in Fig. 3(a). This curve lies well below the experimental  $I_r$ . The discrepancy is attributed to the fact that Eq. (11) underestimates the  $I_r$  values because it uses an approximate expression for  $I_{qp}$ .

In Fig. 3(b), the crosses are the  $I$  values obtained with our procedure. The open circles are the experimental  $I_{qp}$  at  $V_r = 0.1$  mV, the solid and dashed lines are the theoretical  $I_{qp}$  curves corresponding to two different gaps and voltages. They were obtained by the complete integral expression, Eq. (4).<sup>52</sup> We report two curves to allow the gap and voltage values to vary inside our experimental error. The agreement is very good and demonstrates that  $R_{\text{eff}}$ , due to the quasiparticle and quasiparticle-pair interference contributions, is responsible for the return process dissipation at different temperatures. This is a very remarkable result because, if we extrapolate at lower temperature, this means that a very low dissipation is effective in this switching process.

It is worth noticing that our procedure assumes  $\varepsilon = +1$  in Eq. (5). The debate in literature about the sign of  $\varepsilon$  is well known. In our case, a negative choice for the  $\varepsilon$  sign would imply higher  $I$  values from the  $I_r$  fitting, in disagreement with the observed  $I_{qp}$ . Then our measurements seem to indicate a positive sign for  $\varepsilon$ .

Moreover, in this sample, we measured the highest values of the intrinsic junction resistance,  $R_{\text{eff}} = 3.55$  k $\Omega$ . No effects from the biasing circuit were observed.

Unfortunately, with our experimental set-up, it was not possible to perform  $I_r$  measurements for this sample with sufficient sensitivity at temperatures lower than 2 K, where  $I_r$  becomes very small. In fact, our experimental scheme required to bias the JTJ above  $I_c$  before reducing the current to  $I_r$ . Consequently, the current generator limiting resistor (which is also used to read the current) had to be fixed to a relatively small value, thus reducing the return current measurement sensitivity at this temperature.

In this  $J_c$  range, we measured a second sample, namely b, in a wider temperature interval, up to near  $T_c$ . The behavior at low temperatures essentially reproduces the measurements on the previous sample. At high temperature, an interesting change in the  $I_r$  versus  $T$  dependence was observed [see Fig. 4(a)], although the  $R_{qp}$  versus  $T$  dependence is monotone. We explain this behavior taking into account the different temperature dependence of  $J_c$  and  $R_{qp}$  in Eq. (3). In fact, at high temperatures, where the  $I_c$  versus  $T$  dependence is dominant, the whole temperature dependence of  $I_r$  follows a  $I_c^{1/2}$  behavior. Lowering  $T$ ,  $J_c$  rapidly saturates and the whole temperature dependence follows the behavior just observed for sample a. It is worth noticing that Eqs. (3) and (16), and then the RSJ model, work quite well in a very extended temperature interval and that the thermal fluctuations are effective near  $T_c$ . The symbols used in Fig. 4(b), for sample b, are the same as that previously used in Fig. 3(b). Here the experimental  $I_{qp}$  was measured at  $V_r = 0.15$  mV and the quite good agreement extends on the whole temperature range, so confirming that Eq. (15) well describe the effect of thermal fluctuations in the return process.

## B. Intermediate $J_c$ junctions

For sample c,  $I_r$  has been measured at temperatures below 4.2 K, showing an exponential decreasing temperature dependence with a beginning flattening out at  $T = 2$  K, as reported in Fig. 5. This junction is not in the high temperature limit, in fact the ratio  $k_B T / \hbar \omega_p$  is in a range so that neither Eq. (11) nor Eq. (13) are strictly valid. It is then difficult to treat this case.

In Fig. 5, open circles are the experimental  $I_r$  and we have reported the result of Eq. (11) as a solid line and that of Eq. (13) as a dashed line. At a high temperature, the discrepancy with the experimental  $I_r$  values is similar to that for low  $J_c$  junctions and it was possible to apply the fit procedure described above obtaining the noiseless fit values represented by open squares. In the inset, a comparison between the  $I_{qp}$  values obtained as outlined in the previous subsection and the theoretical  $I_{qp}$  values show a quite good agreement

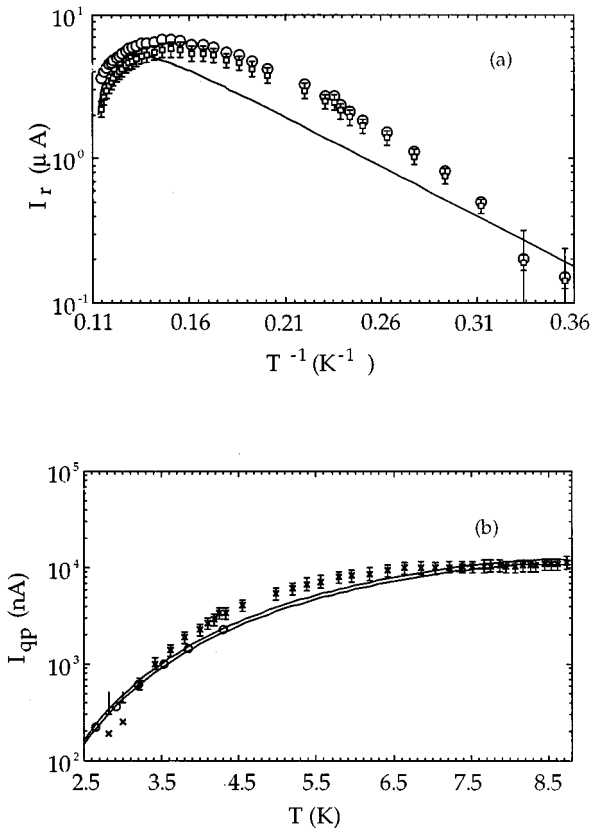


FIG. 4. (a) Semilogarithmic plot of the return current vs the inverse of the temperature for sample b. The symbols are the same reported in Fig. 3(a). (b) Semilogarithmic plot of the quasiparticle current vs the temperature for sample b. The open circles are the measured values of  $I_{qp}$  at  $V=V_r=0.15$  mV. The crosses represent the values of  $I_{qp}^{fit}$ . Error bars, if not reported, are included in the symbols. The solid line is the predicted temperature dependence of  $I_{qp}$  at  $V=V_r$  and  $\Delta=1.425$  mV. The dashed line shows the same dependence with  $V=0.17$  and  $\Delta=1.41$  mV.

down to 2.2 K. At a low temperature, we observed a flattening out of  $I_r$  at values two order of magnitude higher than those predicted from Eq. (13). Is this flattening out due to leakage currents appearing in the junction at low temperature or Eq. (13) underestimate  $I_r$  as Eq. (11) does for the low  $J_c$  junctions? The large discrepancy seems to indicate the former hypothesis.

### C. Higher $J_c$ junctions

In Fig. 6, we report the  $I_r$  versus  $T$  dependence of sample *d* with higher  $J_c$  at  $T < 4.2$  K. In this case, a flattening out effect appeared quite immediately at  $T=3.3$  K. The solid line is the result of Eq. (13). Also in this case, the flattening out values were two order of magnitude larger than the theoretical predictions of Eq. (13). Here, however, we are in the low temperature limit. It is worth noticing that although this sample can be considered of good quality for a higher  $J_c$  junction, the quality is poor if compared with a low  $J_c$  junction. This is reflected in the experimental  $I_{qp}$  versus  $T$  behavior which also exhibited flattening out. This flattening out is probably nothing more than a poor tunnelling bar-

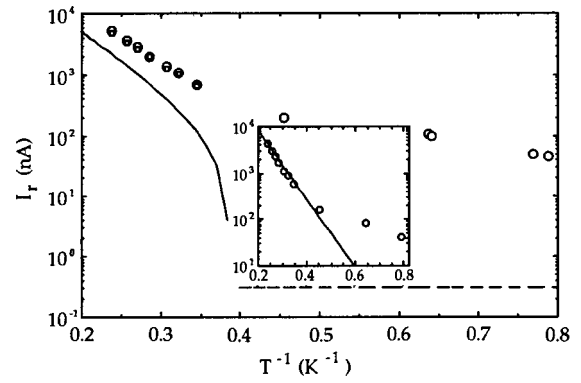


FIG. 5. Semilogarithmic plot of the return and quasiparticle current vs the inverse of the temperature for sample c. The open circles are the measured values of  $I_r$ . The open squares represent the noiseless return current evaluated by Eq. (3). Error bars are included in the symbols. The solid and dashed lines represent the noiseless theory for the return current, respectively, in the high temperature limit, Eq. (11), and in the low temperature limit, Eq. (13). In the inset, semilogarithmic plot of the quasiparticle current vs the inverse of the temperature.

rier effect due to the very thin oxide. Nevertheless, Eq. (13) predicts a  $I_r$  value which is in practice independent on  $T$  at low temperatures even without leakages.

## V. CONCLUSIONS

We have measured the temperature dependence of the return current in high-quality Nb/AlO<sub>x</sub>/Nb Josephson junctions having a wide range of  $J_c$  values. From the experimental data we have obtained  $R_{eff}$ , according to a generalized RSJ model. It must be noticed that  $R_{eff}$  is not simply  $R_{qp}$  because of the presence of the quasiparticle-pair interference term in the junction conductance. Taking into account this difference, it was possible to obtain the corresponding  $R_{qp}$  values and compare them with the measured ones. Our junctions show good agreement between the temperature dependence of these two quantities, inside our experimental error. In particular, low  $J_c$  junctions show agreement down to the

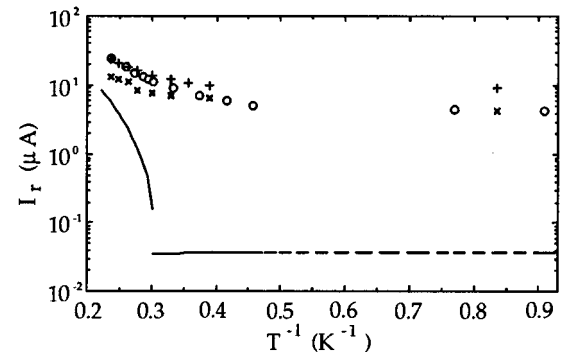


FIG. 6. Semilogarithmic plot of the return and quasiparticle current vs the inverse of the temperature for sample d. The open circles are the measured values of  $I_r$ . The crosses and the  $x$ 's are the measured values of  $I_{qp}$ , respectively, at a voltage  $V=0.5$  and  $V=0.1$  mV. Error bars are included in the symbols. The solid and dashed lines represent the noiseless theory for the return current as in Fig. 5.

minimum temperature  $T=2.1$  K, and no flattening out effects were observed. This has two important consequences:

- (1) low  $J_c$  junctions are typically of the best quality in terms of leakage currents, so that possible flattening out is expected to much lower temperatures than in higher  $J_c$  junctions. Then, a low  $J_c$  junction could reach sufficiently high quasiparticle resistance so that MQC processes can be observed without problems due to high dissipation;
- (2) in low  $J_c$  junctions, we measured the highest  $R_{\text{eff}}$  and we did not observe flattening out. We can then rule out for our experimental configuration any influence of the external bias circuit. This conclusion can be extended to the higher  $J_c$  junctions, because there  $R_{\text{eff}}$  are still smaller and more difficult to shunt.

We also point out that the good quantitative agreement with the experimental  $I_r$  has been obtained in the low  $J_c$  case by using the complete integral expression for the quasiparticle tunnelling current. In the case of junctions with higher  $J_c$ , since we are in the low-temperature limit, it is not obvious to compare the temperature dependence of  $R_{qp}$  with that of  $R_{\text{eff}}$ . In practice, two contemporary effects appear at higher  $J_c$  values, both independently leading to flattening out effects:

- (a) increasing  $J_c$ , the fabrication technology lacks more and more so that leakage currents are expected to appear at some temperature, shunting the intrinsic tunnelling conductance;
- (b) in the low-temperature limit, the CFL theory predicts a temperature independent  $I_r$  value.

We are not able to discriminate between these two possibilities. However, since the observed flattening out occurred at values two order of magnitude larger than the theoretical predictions, this seems either an indication in favor of the first hypothesis or a lack of the theory.

In conclusion, it was claimed that the determination of the dissipation of the junction from the return current data can be considered a reliable estimate of the dissipation for MQC experiments.<sup>14</sup> Although the present work does not represent a confirmation of this hypothesis, we demonstrate that low  $J_c$  Nb/AIO<sub>x</sub>/Nb junctions have an ideal dissipation responsible for the return switching, scaling in temperature according to the BCS exponential behavior down to 2 K. Extrapolation of this temperature dependence to lower temperatures envisages the possibility to reach the desired megaohm range for  $R_{\text{eff}}$  making possible to observe MQC phenomena. Thus, the dissipation obtained from  $I_r$  measurements indicates that Nb/AIO<sub>x</sub>/Nb junctions are ideal candidates for MQC experiments.

Measurements of the decay rate of the zero-voltage state, the resonant macroscopic quantum tunnelling rate between energy levels in the washboard potential well can also provide complementary information about the effective dissipation. These kinds of investigations are very important to obtain a complete picture of the possible dissipation sources responsible of quantum activation, in conditions close to those occurring in the coherent oscillations of the rf-SQUID.

As already mentioned above, Nb/AIO<sub>x</sub>/Nb junctions have the further advantage of entering the quantum regime at relatively higher temperatures, making them interesting devices to be used in all these experiments, which are necessary steps towards a complete characterization of the device which will operate in the final experimental configuration of the MQC experiment.

## ACKNOWLEDGMENTS

R. Monaco and H. Nakagawa are acknowledged for their collaboration in the sample fabrication. We thank A. Barone and A. Leggett for the critical reading of the manuscript.

- <sup>1</sup>A. J. Leggett, Prog. Theor. Phys. Suppl. **69**, 80 (1980).
- <sup>2</sup>S. Chakravarty and A. J. Leggett, Phys. Rev. Lett. **52**, 5 (1984).
- <sup>3</sup>H. Grabert and V. Weiss, Phys. Rev. Lett. **53**, 1787 (1984).
- <sup>4</sup>A. J. Leggett and A. Garg, Phys. Rev. Lett. **54**, 857 (1985).
- <sup>5</sup>L. E. Ballentine, Phys. Rev. Lett. **59**, 1493 (1987).
- <sup>6</sup>A. J. Leggett and A. Garg, Phys. Rev. Lett. **59**, 1621 (1987).
- <sup>7</sup>A. Peres, Phys. Rev. Lett. **61**, 2019 (1988).
- <sup>8</sup>A. J. Leggett and A. Garg, Phys. Rev. Lett. **63**, 2159 (1989).
- <sup>9</sup>J. R. Kirtley, C. D. Tesche, W. J. Gallagher, A. W. Kleinsasser, R. L. Sandstrom, S. I. Raider, and M. P. A. Fisher, Phys. Rev. Lett. **61**, 2372 (1988).
- <sup>10</sup>C. D. Tesche, J. R. Kirtley, W. J. Gallagher, A. W. Kleinsasser, R. L. Sandstrom, S. I. Raider, and M. P. A. Fisher, Proc. 3rd Int. Symp. Foundations of Quantum Mechanics, 1989 (unpublished) 233.
- <sup>11</sup>See, for example, the special issue on Josephson technology in IBM J. Res. Dev. **24**, (1980).
- <sup>12</sup>J. M. Baker and J. H. Magerlein, J. Appl. Phys. **54**, 2556 (1983).
- <sup>13</sup>J. H. Magerlein, J. Appl. Phys. **54**, 2569 (1983).
- <sup>14</sup>Y. C. Chen, M. P. A. Fisher, and A. J. Leggett, J. Appl. Phys. **64**, 3119 (1988).
- <sup>15</sup>A. O. Caldeira and A. J. Leggett, Phys. Rev. Lett. **46**, 211 (1981).
- <sup>16</sup>T. A. Fulton and L. N. Dunkelberger, Phys. Rev. B **9**, 4760 (1974).
- <sup>17</sup>L. D. Jackel, J. P. Gordon, E. L. Hu, R. E. Howard, L. A. Fetter, D. M. Tennant, R. W. Epworth, and J. Kurkijarvi, Phys. Rev. Lett. **47**, 997 (1981).
- <sup>18</sup>R. F. Voss and R. A. Webb, Phys. Rev. Lett. **47**, 265 (1981).
- <sup>19</sup>S. Washburn, R. A. Webb, R. F. Voss, and S. M. Faris, Phys. Rev. Lett. **54**, 2712 (1985).
- <sup>20</sup>P. Silvestrini, O. Liengme, and K. E. Gray, Phys. Rev. B **37**, 1525 (1988).
- <sup>21</sup>P. Silvestrini, S. Pagano, R. Cristiano, O. Liengme, and K. E. Gray, Phys. Rev. Lett. **60**, 844 (1988).
- <sup>22</sup>P. Silvestrini, J. Appl. Phys. **68**, 663 (1990).
- <sup>23</sup>P. Silvestrini, Phys. Rev. B **46**, 5470 (1992).
- <sup>24</sup>M. H. Devoret, J. M. Martinis, D. Esteve, and J. Clarke, Phys. Rev. Lett. **53**, 1260 (1984).
- <sup>25</sup>M. H. Devoret, J. M. Martinis, and J. Clarke, Phys. Rev. Lett. **55**, 1908 (1985).
- <sup>26</sup>J. M. Martinis, M. H. Devoret, and J. Clarke, Phys. Rev. B **35**, 4682 (1987).
- <sup>27</sup>A. N. Cleland, J. M. Martinis, and J. Clarke, Phys. Rev. B **37**, 5950 (1988).
- <sup>28</sup>E. Turlot, D. Esteve, C. Urbina, J. M. Martinis, M. H. Devoret, S. Linkwitz, and H. Grabert, Phys. Rev. Lett. **62**, 1788 (1989).
- <sup>29</sup>J. M. Martinis and R. Kautz, Phys. Rev. Lett. **63**, 1507 (1989).
- <sup>30</sup>R. Kautz and J. M. Martinis, Phys. Rev. B **42**, 9903 (1990).
- <sup>31</sup>C. Cosmelli, G. Diambri-Palazzi, F. Chiarello, A. Costantini, M. G. Castellano, R. Leoni, G. Torrioli, P. Carelli, R. Cristiano, and L. Frunzio, Inst. Phys. Conf. Ser. **148**, 1323 (1995).
- <sup>32</sup>H. A. Kramers, Physica **7**, 284 (1940).
- <sup>33</sup>H. Grabert, V. Weiss, and P. Hanggi, Phys. Rev. Lett. **52**, 2193 (1982).
- <sup>34</sup>M. Buttiker, E. P. Harris, and R. Landauer, Phys. Rev. B **28**, 1268 (1983).
- <sup>35</sup>M. Buttiker and R. Landauer, Phys. Rev. B **30**, 1551 (1984).
- <sup>36</sup>S. Han, J. Lapointe, and J. E. Lukens, Phys. Rev. Lett. **66**, 810 (1991).
- <sup>37</sup>S. Han, J. Lapointe, and J. E. Lukens, Phys. Rev. B **46**, 6338 (1992).
- <sup>38</sup>R. Rouse, S. Han, and J. E. Lukens, Phys. Rev. Lett. **66**, 1614 (1995).
- <sup>39</sup>E. Ben-Jacob, D. J. Bergman, B. J. Matkowsky, and Z. Schuss, Phys. Rev. A **26**, 2805 (1982).



- <sup>40</sup>H. D. Vollmer and H. Risken, *Z. Phys. B* **37**, 343 (1980).
- <sup>41</sup>V. I. Mel'nikov, *Zh. Eksp. Teor. Fiz.* **88**, 1429 (1985) [*JETP* **61**, 855 (1985)].
- <sup>42</sup>R. Cristiano and P. Silvestrini, *J. Appl. Phys.* **59**, 1401 (1986).
- <sup>43</sup>R. Cristiano and P. Silvestrini, *IEEE Trans. Magn.* **23**, 771 (1987).
- <sup>44</sup>R. Cristiano, S. Pagano, and P. Silvestrini, *IEEE Trans. Magn.* **25**, 1416 (1988).
- <sup>45</sup>R. Cristiano and P. Silvestrini, *Phys. Lett. A* **133**, 347 (1988).
- <sup>46</sup>A. T. Johnson, C. J. Lobb, and M. Tinkham, *Phys. Rev. Lett.* **65**, 1263 (1990).
- <sup>47</sup>D. E. McCumber, *J. Appl. Phys.* **39**, 3113 (1968).
- <sup>48</sup>A. Barone and G. Paternò, *Physics and Application of the Josephson Effect* (Wiley, New York, 1982).
- <sup>49</sup>R. Monaco, R. Cristiano, L. Frunzio, and C. Nappi, *J. Appl. Phys.* **71**, 1888 (1992).
- <sup>50</sup>R. Cristiano, E. Esposito, L. Frunzio, S. Pagano, A. Barone, G. Peluso, G. Pepe, H. Akoh, H. Nakagawa, and S. Takada, *J. Appl. Phys.* **75**, 5210 (1994).
- <sup>51</sup>M. G. Castellano, R. Leoni, G. Torrioli, F. Chiarello, C. Cosmelli, A. Costantini, G. Diambri-Palazzi, P. Carelli, R. Cristiano, and L. Frunzio, *J. Appl. Phys.* **80**, 2922 (1996).
- <sup>52</sup>R. Cristiano, L. Frunzio, and C. Nappi, *Nuovo Cimento D* **14**, 395 (1992).